



Diffusion Barrier Characteristics of Ni-NbO_x Composite Electrodeposits for Liquid In-Sn Solder Interconnects

Jing Wang,^{a,*} Geoffrey D. Wilcox,^a Roger J. Mortimer,^b Changqing Liu,^c and Mark A. Ashworth^a

^aDepartment of Materials, Loughborough University, Loughborough, Leicestershire LE11 3TU, United Kingdom

^bDepartment of Chemistry, Loughborough University, Loughborough, Leicestershire LE11 3TU, United Kingdom

^cWolfson School of Mechanical and Manufacturing Engineering, Loughborough University, Loughborough, Leicestershire LE11 3TU, United Kingdom

The control of interfacial microstructural stability is of utmost importance to the reliability of liquid solder interconnects in high temperature electronic assemblies. This is primarily due to excessive intermetallic compounds (IMCs) that can form and continuously grow during high temperature operation, which renders conventional barrier metallizations inadequate. With the intention of reducing such excessive IMC growth, electrically conducting, NbO_x containing Ni coatings were developed using electrodeposition and were assessed as solder diffusion barrier layers in terms of their electrical conductivity and barrier property. The present work adopts a novel electrochemical route to produce Ni-NbO_x composite coatings of good uniformity, compactness and purity, from non-aqueous glycol-based electrolytes consisting of NiCl₂ and NbCl₅ as metal precursors. The effects of cathodic current density and NaBH₄ concentrations on the surface morphology, composition and thickness of the coatings were examined. Increased NaBH₄ concentrations were found to elevate the maximum deposit thickness (above 10 μm), although these led to a reduction in the co-deposited Nb content. The composite coatings generally exhibited good electrical conductivity. The reaction between a liquid 52In-48Sn solder and Ni-NbO_x, with Nb contents up to 6 at.%, was studied at 200°C. The results indicate that, Ni-NbO_x with sufficient layer thickness and higher Nb content, offered longer service lifetime. Nb enrichment was generally observed at or close to the reaction front after high temperature storage which suggests evident effectiveness of the enhanced diffusion barrier characteristics. A mechanism for the role of Nb as a barrier performance enhancer was postulated.

© The Author(s) 2015. Published by ECS. This is an open access article distributed under the terms of the Creative Commons Attribution 4.0 License (CC BY, <http://creativecommons.org/licenses/by/4.0/>), which permits unrestricted reuse of the work in any medium, provided the original work is properly cited. [DOI: 10.1149/2.0331504jes] All rights reserved.

Manuscript submitted December 8, 2014; revised manuscript received January 6, 2015. Published January 22, 2015. This was Paper 1710 presented at the Cancun, Mexico, Meeting of the Society, October 5–9, 2014.

For electronic assemblies operated in high temperature environments such as those in aero-engine, oil well and geothermal drilling applications, the high operating temperatures (usually above 200°C) far exceed the conventional design limits (up to 125°C) of consumer electronic products and have resulted in a demand to generate more confidence in the performance and reliability of the solder interconnects. This is mainly due to strain hardening induced in the solder joints under the combined high temperature and mechanical vibration, leading to premature joint failure. The concept of a “liquid solder joint” has been put forward,^{1,2} which utilizes a solder (e.g. Sn-In) with a melting point *below* the operation temperature, whereby the regular re-melting of the solder during the service life can effectively remove any accumulated thermal stress and associated progressive deterioration of the solder properties. However, the accelerated formation and growth of undesirable Sn-Cu intermetallic compounds (IMCs) at the interface between the Sn-based solder and Cu-based component has posed a considerable threat to the joint reliability as they tend to instigate brittle failure. This has rendered the conventional solder barrier metallizations (e.g. electrolytic Ni³ and electroless Ni-P⁴) inadequate. A 1 μm thick Nb metal layer has been found to be a promising replacement, which is effective not only in preventing excessive Sn-Cu IMC formation, but also in providing good adhesion through formation of a self-limiting Sn-Nb IMC layer.^{1,2} However, Nb metal cannot be electrodeposited from aqueous solutions, whilst its currently available preparation method, physical vapor deposition (PVD), suffers from low productivity and poor selectivity in the substrate materials. The present work, therefore, seeks to co-deposit Ni with Nb using an electrodeposition approach, in an attempt to improve the barrier performance of electrolytic Ni barrier metallization. It has been noted that by co-depositing Ni-P with W, certain improvement in the diffusion barrier capability of the former has been promoted.⁵ It is of interest, therefore, to examine the possible role of Nb as a diffusion barrier enhancer for Ni layers.

In our previous paper,⁶ we have explored a novel electrodeposition route for the preparation of Ni-NbO_x composite diffusion barrier

layers from non-aqueous, glycol-based electrolytes. Due to the high affinity of Nb to O, Nb could not be electrochemically reduced to its metal state. The NbO_x species was electrolytically generated in situ in the diffusion layer so that their subsequent occlusion into the growing deposit allows for highly uniform and repeatable dispersion of Nb within the Ni matrix (i.e. without appreciable phase segregation). The coating thickness, however, is found to have a maximum at 2–3 μm, which may render these coatings insufficient for diffusion barrier applications of high temperature electronics. The present study seeks to elevate the thickness of these Nb-containing deposits, through manipulation of the electroplating bath chemistry (e.g. adjusting the bath acidity by varying the concentration of a chemical reducing agent, NaBH₄). This also facilitates a better understanding of the underlying mechanism of the Ni-Nb double salt electrodeposition system. The electrical conductivity and diffusion barrier efficacy of the Ni-NbO_x deposited samples at Nb contents ranging from 0.6 to 6 at.%, have also been investigated. The latter aspect was achieved by examining the reaction behaviors of the Ni-NbO_x layer with a molten 52In-48Sn solder at 200°C for various storage periods. The reacted Ni-NbO_x/In-Sn diffusion couples were cross-sectioned and characterized using SEM/EDX analysis.

Experimental

NbCl₅ (99.9%, Sigma Aldrich), NiCl₂ hexahydrate (NiCl₂ · 6H₂O) (99%, Fisher), NaBH₄ (99.99%, Sigma Aldrich) and propylene glycol (HO-CH(CH₃)CH₂-OH) (99.5%, SAFC) were utilized as received. The procedure of making the electrolyte was reported by the authors previously in Ref. 6. Table I summarizes the formulation of the Ni-Nb electrodeposition baths. Propylene glycol was utilized as the supporting medium due to its high solubility of NbCl₅ and NiCl₂, excellent buoyancy of electrolytically formed Nb oxides, good electrochemical stability and thermal stability. Variations in the NaBH₄ (a bath acidity modifier) concentrations and cathodic current density were made to examine their effect on the co-deposited Nb content and cathodic current efficiency (coating thickness).

*Electrochemical Society Student Member.

^zE-mail: J.Wang@lboro.ac.uk

Table I. Formulations of Ni-Nb electrodeposition electrolytes (g/L (M)).

| Compounds | Bath A | Bath B | Bath C |
|---------------------------------------|----------------|----------------|----------------|
| Propylene glycol (PG) | 1036.0 (13.63) | 1036.0 (13.63) | 1036.0 (13.63) |
| NbCl ₅ | 147.2 (0.54) | 147.2 (0.54) | 147.2 (0.54) |
| NiCl ₂ · 6H ₂ O | 4.26 (0.018) | 4.26 (0.018) | 4.26 (0.018) |
| NaBH ₄ | 20.6 (0.54) | 41.2 (1.08) | 61.8 (1.62) |

Electrodeposition was conducted using copper substrates (99.9%, 100 μm thickness), with an electroplated area of 1 cm × 1 cm. For pre-treatment, the substrate was ultrasonically cleaned for 3 min in acetone, pickled for 1 min in a 20% v/v solution of H₂SO₄ (S.G.: 1.83) at ambient temperature (~20°C), rinsed in deionized water and dried under compressed air. The anode material was a niobium metal sheet (99.9%, 500 μm thickness), which was utilized immediately after a manual grinding step using silicon carbide paper (240 grit). Direct current galvanostatic deposition was performed using a QPX 1200S DC power supply (Thurlby Thandar Instruments) at 100°C under magnetic stirring agitation at 240 rpm. Current densities ranging from 30 to 150 mA/cm² were applied with equivalent electric charge passed.

After electrodeposition, the Ni-NbO_x deposited samples were thoroughly rinsed using deionized water followed by acetone and dried under a hot air stream. Electrical resistance was assessed by four-point probe using a Keithley 2440 5A Source meter. Eutectic 52In-48Sn solder paste (Indalloy 1E, Ni-compatible flux NC-SMQ80, Indium Corporation, USA) was manually deposited onto the coated sample surface through a syringe, with an average solder thickness of ca. 2 mm, and reflowed at 200°C in air for 1 min. The samples were again cleaned using deionized water and acetone before storage in an ambient oven at 200°C for periods up to 2 weeks.

FEG-SEM/EDS analysis, using a Carl Zeiss Leo 1530 VP FEG SEM equipped with Oxford Instruments X-Max 80 mm² EDX detector, was conducted to examine the surface and cross-sectional morphology and composition of the as-deposited samples, and also to reveal the In-Sn/Ni-NbO_x interfacial microstructure of the specimens after diffusion tests. Deposit composition was assessed in the central region in at least three different locations at ×1000 magnification by EDX area analysis (unless otherwise noted). The deposit thickness was estimated directly from cross-sectional views. Cross-sections were prepared by mounting in resin, grinding using silicon carbide papers (240–1200 grit) and polishing using 6 μm and 3 μm diamond suspensions. Final polishing was conducted using colloidal silica (0.04 μm) suspension. Before SEM observation, the cross-sectioned specimens were carbon coated to ensure good electrical conduction.

Results and Discussion

Effect of NaBH₄ on the Ni-NbO_x electrodeposition.— Representative surface morphologies of as-deposited Ni-NbO_x, with variations in the NaBH₄ bath concentrations and in the cathodic current density from 30 to 150 mA/cm², are illustrated in Fig. 1. For all the three baths (A, B & C), increasing the current density from 30 to 150 mA/cm² was generally found to result in a reduction in the average dimension of deposit surface features, most of which appeared to be granular. This is attributable to an increasing preference for grain nucleation, rather than growth of the existing grains. At 150 mA/cm², discrete, coral-like developments were observed for both baths B & C (with relatively high NaBH₄ concentrations). This is thought to be due to mass transfer being the rate controlling step, when, at large over-potential, the consumption of the Ni ions in the diffusion layer exceeded that of their replenishment, encouraging localized crystal growth out of the diffusion layer. With increasing NaBH₄ concentrations, a coarsening of the deposit surface features was generally observed. For example at 30 mA/cm², with increasing NaBH₄ concentrations from 0.54 M (bath A) to 1.62 M (bath C), the feature size increased from submicron (Fig. 1a) to a few micrometres (Fig. 1i).

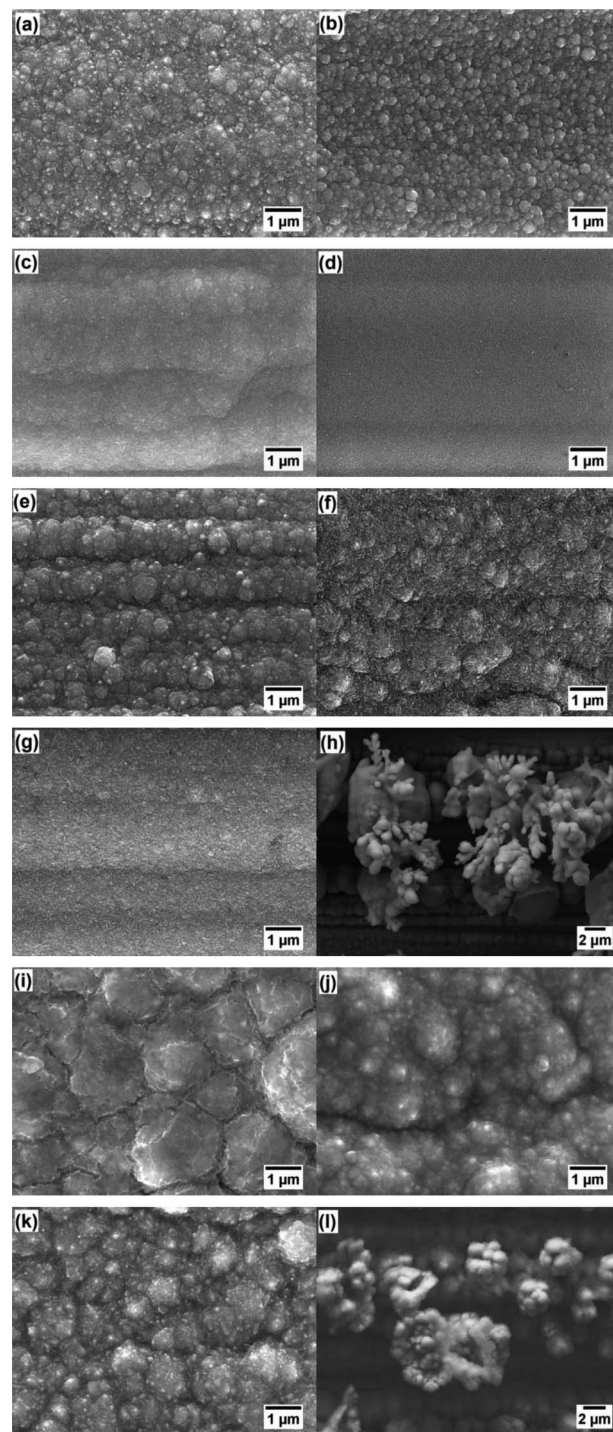


Figure 1. SEM images showing the representative surface morphology of Ni-Nb electrodeposited at 100°C & 240 rpm from bath A (a-d), bath B (e-h) & bath C (i-l) at a current density of 30 (a, e, i), 50 (b, f, j), 100 (c, g, k) and 150 mA/cm² (d, h, l) respectively with an equivalent charge passage of 360 C per cm².

The percentage of Nb in the deposits as well as the average deposit thickness is presented in Fig. 2. Except for the deposits prepared at 150 mA/cm² from baths B and C, the Ni-NbO_x deposits were generally found to be compact and uniform. It was observed that those deposits with relatively small surface features (i.e. obtained at high cathodic current densities and low NaBH₄ concentrations) tended to exhibit relatively high Nb contents (Fig. 2a) and low deposit thicknesses (Fig. 2b). With increasing NaBH₄ concentrations from 0.54 M (bath

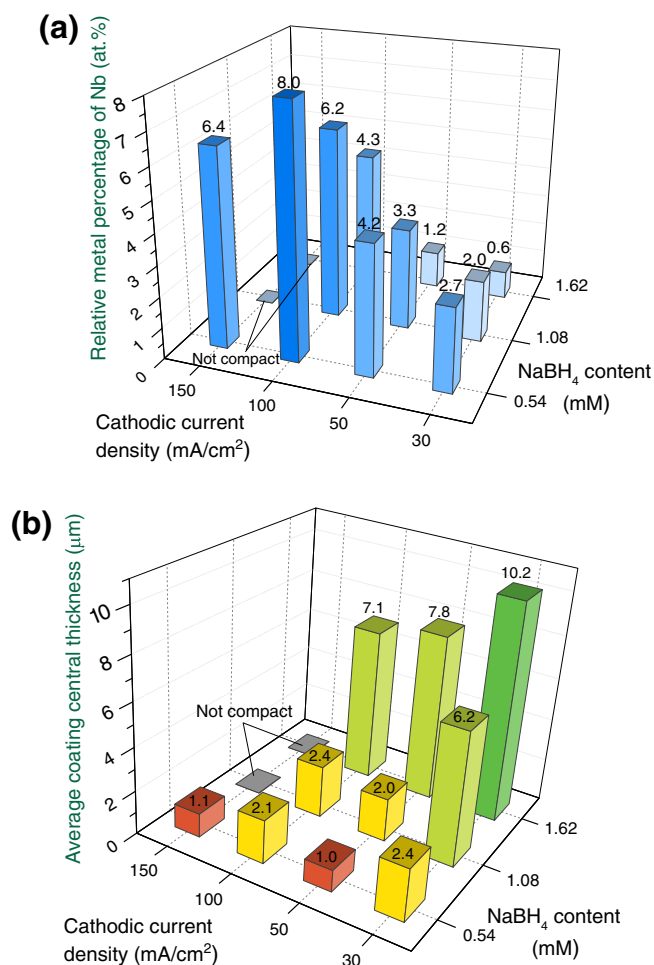


Figure 2. Bar charts showing the variations in the a) relative metal percentage of Nb in the Ni-NbO_x deposits and in b) average deposit thickness with cathodic current density and NaBH₄ concentration in the bath (revealed by cross sectioning and polishing).

A) through 1.08 M (bath B) to 1.62 M (bath C), the apparent pH of the bath saw a rise from ~ 0.6 through 2.5 to 5.2 at 100 (±3)°C. This suggests that NaBH₄ is reducing the proton concentration in the electrolyte, and leads to the presumption that, the increase in the bath pH results in reduced hydrogen evolution at the cathode, which elevates the partial current density of Ni reduction but not necessarily the Nb co-deposition. This explains a reduction in the co-deposited NbO_x content with increased NaBH₄ concentrations. Also, all the three baths remained acidic after NaBH₄ additions, and subsequently maintained free of dark coloration upon NiCl₂ additions. These signify that BH₄⁻ ions had been completely consumed from their reaction with H⁺ ions, which otherwise would reduce Ni²⁺ ions thereafter forming black nickel borides precipitates. This partially denied the possible occurrence of an electroless Ni deposition in the present study, which is further corroborated by the observed absence of any deposition when no current density was applied.

It is noteworthy that the deposit thickness shown in Fig. 2b represents the maximum that can be obtained for each set of conditions, since a halving of the electric charge passage (i.e. 180 C per cm²) has been found to yield deposits with comparable coating thickness and surface morphology. The average maximum thickness of these deposits generally saw a decrease with increased co-deposited NbO_x content. This may suggest that, during electrodeposition, the growth of uniform deposit ceased at a certain point presumably due to loss of the adherence with the Cu substrate, the onset of which is very likely affected by the NbO_x content already present in the deposits. Based

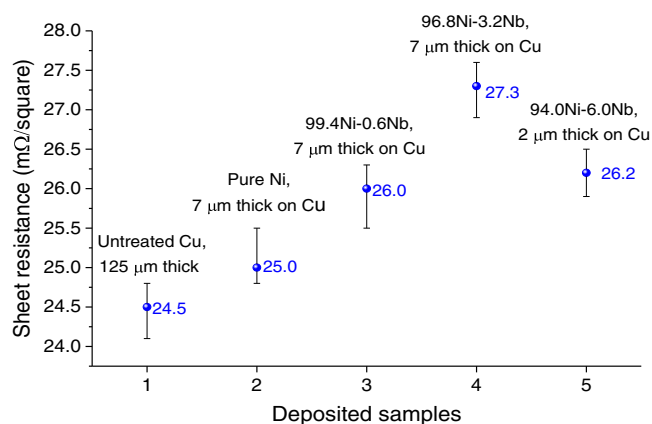


Figure 3. Graph showing the average sheet resistance of untreated Cu sheet and Ni-based, deposited samples measured using the four point probe method.

on this reasoning, the NaBH₄ additions reduce the amount of NbO_x to be co-deposited and hence elevate the maximum deposit thickness.

Therefore, it can be concluded that, there is a trade-off between high Nb content and large deposit thickness for the production of Ni-NbO_x deposits, with the relatively large coating thickness obtained at high NaBH₄ concentration and low cathodic current density whilst the relatively high Nb content obtained at low NaBH₄ concentration and high current density.

Electrical conductivity assessment of Ni-NbO_x electrodeposits.— The introduction of NbO_x into the Ni metal coating may raise concerns over the possible degradation of its electrical conductivity. To examine this, the sheet resistance of pure Ni and Ni-NbO_x deposited samples was measured and plotted in Fig. 3. 7 µm thick pure Ni on Cu electrodeposited at 12 mA/cm² from Bath C showed a ca. 0.5 mΩ increase in the sheet resistance compared with that of the neat Cu substrate (24.5 mΩ); whilst the Ni-NbO_x deposited samples with Nb content ranging from 0.6 to 6.0 at.% showed an increase (of up to 9.2%) in the sheet electrical resistance compared with their pure Ni counterpart. Such magnitudes of decrease in the electrical conductivity can be tolerated for the diffusion barrier application. In our previous paper,⁶ we have demonstrated that both the Nb and O elements are fairly uniformly distributed within the Ni matrix of these composite coatings. Therefore, the thin film electrical conductivity is likely provided by the Ni component, even though the universal presence of NbO_x clusters may somewhat reduce the electrical conductivity capability.

Liquid state interfacial reaction.— Ni-NbO_x deposited samples with different Nb contents of up to 6 at.% were selected for diffusion study with molten Sn-In solder at 200°C for periods of up to 2 weeks. It should be noted that, because of the aforementioned trade-off between high Nb content and large coating thickness for the production of these composite coatings, it becomes impossible to compare samples with different Nb contents but the same coating thickness. Therefore, two groups of deposits with thicknesses of 7 and 2 µm, were examined, and are summarized in Table II. End-of-life failure was defined as

Table II. Summary of the lifetime of pure Ni and Ni-NbO_x barrier layers in contact with molten 52In-48Sn solder at 200°C.

| Coating Thickness | Coating composition (metal atomic percentage) | Lifetime |
|-------------------|---|----------|
| 7 µm | Pure Ni | <48 hrs |
| | 99.4Ni-0.6Nb | <72 hrs |
| | 96.8Ni-3.2Nb | <192 hrs |
| 2 µm | Pure Ni | <3 hrs |
| | 94.0Ni-6.0Nb | <3 hrs |

when the Sn-In solder starts to penetrate through the Ni-based barrier layer into the Cu substrate. The deposit thickness appears to have the most significant influence over the barrier efficacy of the Ni-based layers, since both the 2 μm thick, pure Ni and 94Ni-6NbO_x layers failed within 3 hours, whereas the 7 μm thick pure Ni failed within 48 hours and the similarly thick Ni-NbO_x survived for even longer periods (up to 192 hours). Another factor which showed considerable effect was the co-deposited NbO_x content. With increasing Nb content from 0 through 0.6 to 3.2 at.%, the lifetime of the barrier layers was extended from 48 to 72 hrs, and further to 192 hrs. The reason that the deposit with a high Nb loading (i.e. 94Ni-6NbO_x) failed within 3 hrs, is largely attributed to its low thickness (2 μm), as well as to the cracks arising from interaction with the molten solder. The latter aspect will be considered in more detail later.

Figure 4 shows representative interfacial structures and the IMCs formed between In-Sn solder and the Ni-based barrier layers after high temperature storage at 200°C. It was found that there were generally two types of IMCs growing simultaneously, those IMCs growing at the solder side into the solder bulk, as well as those forming on the Ni-based barrier side. For the 7 μm thick, pure Ni and 99.4Ni-0.6NbO_x (Figs. 4a and 4b), the IMCs formed at the solder side were mostly well-faceted, some of which had spalled and migrated from the solder/IMC interface into the bulk of the molten solder after 72 hrs at 200°C. EDX point analyses indicate these IMC grains contain Ni, In and Sn, in various compositions. This is because the Ni-In-Sn system has been reported to have no ternary IMCs, but binary compounds with excessive ternary solubility.⁷ Little Nb content was detected within these IMC grains, which implies that Nb was not directly involved in the intermetallic formation. For the 96.8Ni-3.2NbO_x (Fig. 4c), most of the Ni-In-Sn IMC structures growing into the solder were still attached to the solder/IMC interface forming a relatively continuous IMC layer, without having spalled into the bulk solder after 216 hours even when the barrier layer had been penetrated. A barrier layer with such a continuous intermetallic layer on top is thought to be more effective in retarding inter-diffusion of Ni, In and Sn atoms, when compared to one with IMCs continuously forming and spalling into the molten solder. However, the 94.0Ni-6.0NbO_x layer did not exhibit such IMC characteristics and showed spalled and discrete Ni-In-Sn IMCs with a faceted geometry (Fig. 4d), presumably due to its insufficient thickness (2 μm). Another reason is the presence of cracks in this high Nb content layer, as is revealed from the cross-section (Fig. 4d) and also from the top view (Fig. 5). Figure 5 shows the exposed surface morphology of a 2 μm thick, 94.0Ni-6.0NbO_x layer that reacted with molten Sn-In solder at 200°C for 5 hours after chemical stripping away the overlying solder using an aqueous, o-nitrophenol/NaOH solution (50 g/L NaOH, 35 g/L o-nitrophenol). In Fig. 5, a network of cracks was observed on the composite barrier layer, which appeared to provide a direct pathway for molten solder ingress into the underlying Cu substrate, giving rise to preferential Sn-In-Cu IMC formation (in various proportions suggested from EDX point analysis) through the cracks and hence premature failure. It is noteworthy that, the unsoldered region of the 94.0Ni-6.0NbO_x layer did not show any cracks, which implies the cracking might have been initiated by interaction with the molten solder.

From the present investigation, it is evident that the addition of the NbO_x content up to 3.2 at.% into the Ni layer, in conjunction with a deposit thickness of at least 7 μm , enhanced its barrier efficacy. In order to understand the exact role of Nb as a barrier performance enhancer, EDX compositional analysis across the interface has been conducted on the soldered, Ni-NbO_x deposited samples for different Nb contents. As illustrated in Fig. 6, five zones could be identified across the interface of the 99.4Ni-0.6NbO_x deposited sample after storage at 200°C for 72 hrs: I) Cu substrate, II) un-consumed Ni-NbO_x layer, III) consumed barrier layer with elevated Nb content (1 at.% Nb), IV) consumed barrier layer depleted in Nb (up to 0.2 at.% Nb) and V) IMCs growing at the solder side (assuming that the IV/V interface represents the position of the original interface between the barrier layer and solder). From the consumed barrier region (Zones III & IV), the enrichment of Nb was found in the front

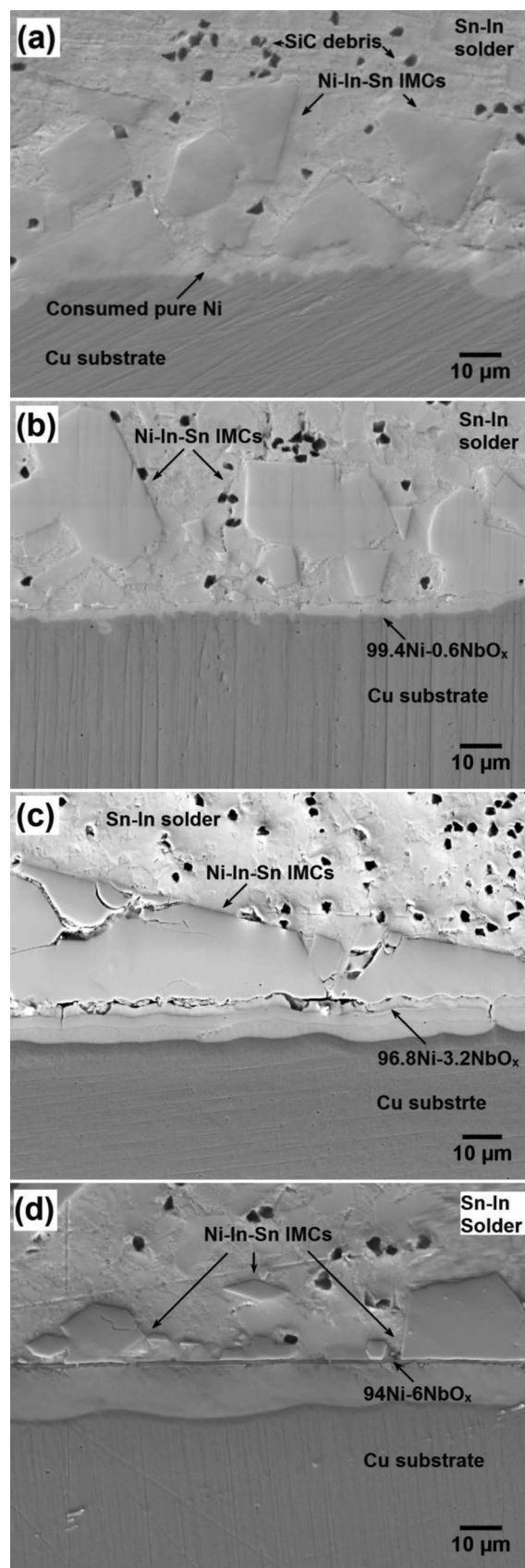


Figure 4. SEM images showing the representative interfacial microstructure of pure Ni and Ni-NbO_x deposited samples after reaction with molten 52In-48Sn: a) 7 μm thick, pure Ni for 72 hours and b) 7 μm thick, 99.4Ni-0.6Nb for 72 hours, c) 7 μm thick, 96.8Ni-3.2Nb for 216 hours and d) 2 μm thick, 94.0Ni-6.0Nb for 9 hours.

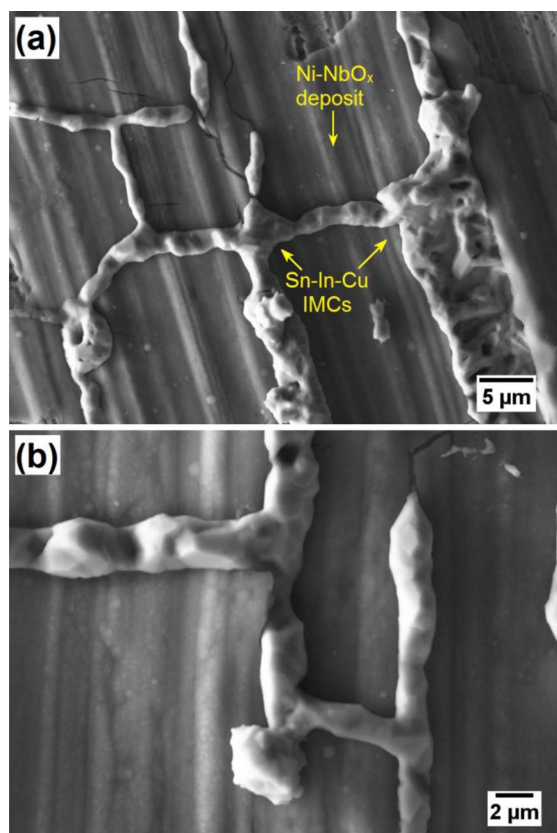


Figure 5. SEM images showing the representative surface morphology of a 2 μm thick 94.0Ni-6.0NbO_x deposited sample that reacted with molten Sn-In solder at 200°C for 5 hours after chemical stripping away the solder (the parallel ridges on the Ni-NbO_x deposits are attributed to the rolling process carried out to fabricate the copper substrate sheet).

of the reaction between molten solder and the barrier, which suggests that the Nb species had migrated with Sn and In (i.e. solid state diffusion) during the Sn-Ni-In IMC formation. It is believed that, the enhancing effect of Nb on the barrier property of the Ni-based layer arises, at least partially, from such a re-distribution of Nb at the reaction front. TEM crystallographic characterization of the interfacial structure is currently ongoing to investigate whether metallic Nb was present in solution within the IMC or was incorporated as discrete NbO_x compounds within the Ni-In-Sn IMCs. Also from Fig. 6b, the reacted region (including Zones III, IV & V) showed fairly constant compositions, at around 46Sn-29In-25Ni for Zones III & IV and at around 47Sn-31In-22Ni for Zone V.

With the codeposited Nb content increased from 0.6 to 3.2 at.%, the 7 μm thick Ni-NbO_x layer saw an extension of the barrier lifetime from 72 to 192 hrs. Figure 7 presents the interfacial microstructure of a 7 μm thick, 96.8Ni-3.2NbO_x deposited sample after reaction with molten Sn-In solder at 200°C for 192 hrs. Once more, five zones could be identified across the interface: I) Cu substrate, II) un-consumed Ni-NbO_x layer, III) consumed barrier layer with slightly elevated Nb content (~ 4.5 at.% Nb), IV) consumed barrier layer with elevated Nb content (~ 10 at.% Nb) and V) IMCs growing at the solder side. The enrichment of Nb in the consumed barrier layer (Zones III & IV) was evident, which was, nevertheless, not necessarily accompanied by the presence of a Nb depleted region, as observed for the 99.4Ni-0.6NbO_x sample. This may imply there is shrinkage of the diffusion barrier, as Ni, the major component of the barrier layer, diffuses into the solder side to form IMCs. This assumption is corroborated by the observations from the 94.0Ni-6.0NbO_x sample shown later. Also, even though the Nb content in the reaction front (i.e. Zone III) is elevated (~ 4.5 at.%) when compared with that in the remaining barrier

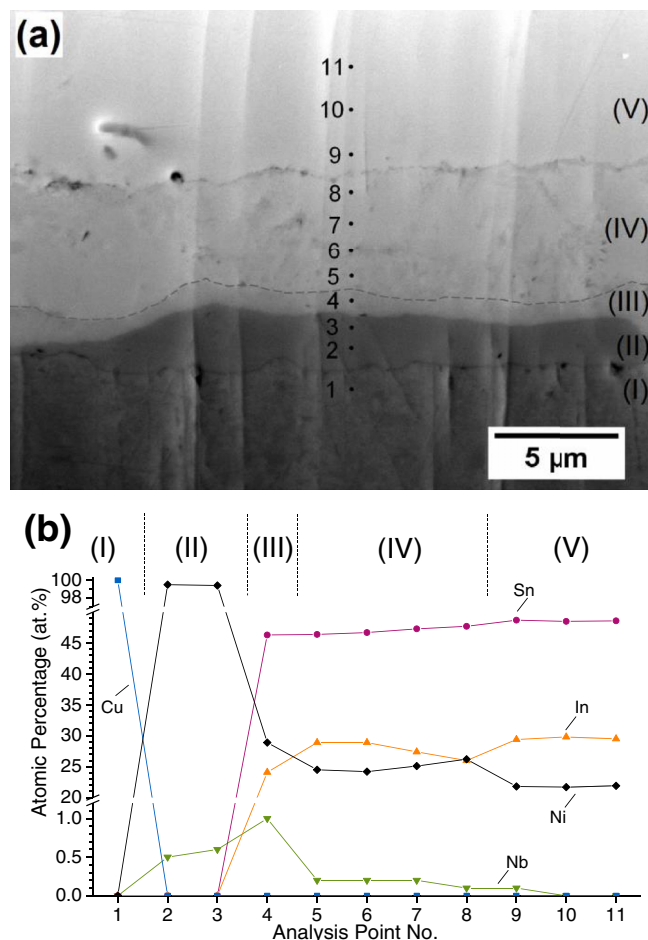


Figure 6. a) SEM image showing the representative interfacial microstructure of a 99.4Ni-0.6Nb deposited samples after reaction with molten Sn-In solder at 200°C for 72 hours and b) a plot showing the EDX point analysis results indicated in a).

layer (~ 3.2 at.%), it can be seen that Zone IV contained the highest Nb content (~ 10 at.%) of all the zones. In Zone IV, the atomic percentage of In was also elevated (~ 45 at.%), as compared to that of the adjacent zones (down to ~ 22 at.% In in both Zones III & V). The atomic ratio of In to Nb was ca. 45:10 in this region. Such enrichments of Nb and In in Zone IV were also reflected in the X-ray maps of the corresponding region, as illustrated in Fig. 8. These results imply that In, from the molten solder, may have a higher affinity for the Nb species present in the barrier layer than Sn. However, the Nb atoms did not appear to migrate significantly with the reaction front, which eventually resulted in Zone III with Nb contents intermediate between that of Zone II and Zone IV. We have demonstrated in the previous paper⁶ that, the composition of the Ni-NbO_x layer across the deposit thickness was almost constant, with only slight compositional fluctuations. Therefore, the present multi-layer interfacial structure is likely to be an intermediate stage during the redistribution of the Nb species, as the diffusion rate of the O-bonded and presumably In-associated Nb may be slower than that of Sn. Besides, the IMCs formed at the solder side (Zone V) exhibited a composition comparable to that of the Zone V from the 99.4Ni-0.6NbO_x sample, which is also similar to that observed from the interface of a pure Ni layer. This suggests that Nb does not necessarily alter the composition of the Sn-Ni-In IMCs growing at the solder side. Nb is more likely to retard the consumption of the Ni-based layer, presumably by slowing down the inter-diffusion of Sn, In and Ni atoms.

With the codeposited Nb content further increased from 6.0 at.%, the Ni-NbO_x layer suffered from a limited thickness (~ 2 μm) and

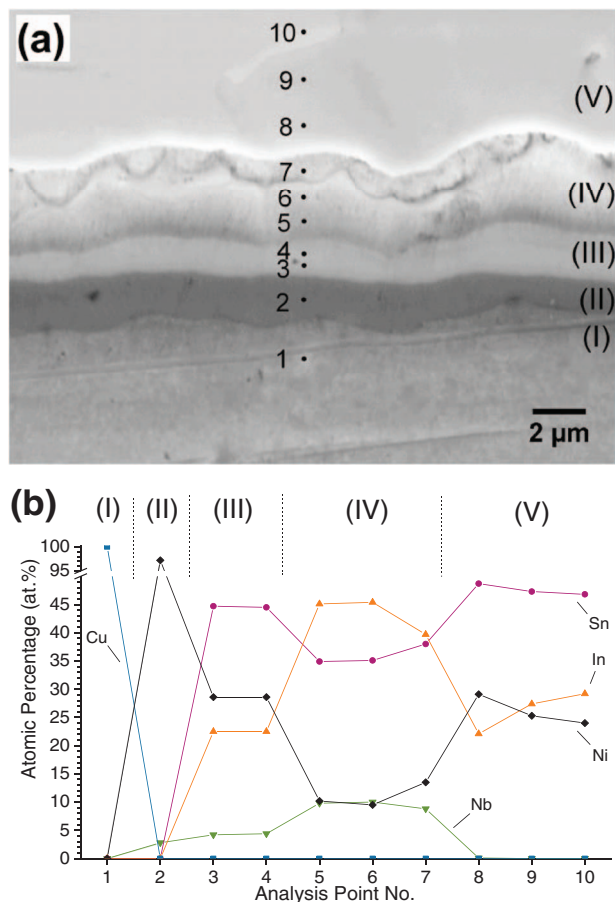


Figure 7. a) SEM image showing the interfacial microstructure of a 96.8Ni-3.2Nb deposited samples after reaction with molten Sn-In solder at 200°C for 192 hours and b) a plot showing the EDX point analysis results indicated in a).

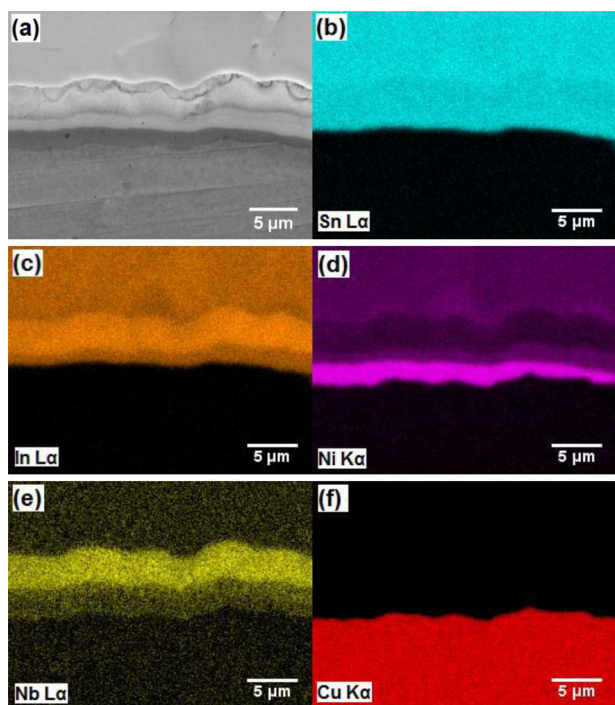


Figure 8. a) SEM image showing the interfacial microstructure of a 96.8Ni-3.2Nb deposited samples after reaction with molten Sn-In solder at 200°C for 192 hours and the corresponding X-ray maps showing b) Sn L α , c) In L α , d) Ni K α , e), Nb L α , and f) Cu K α .

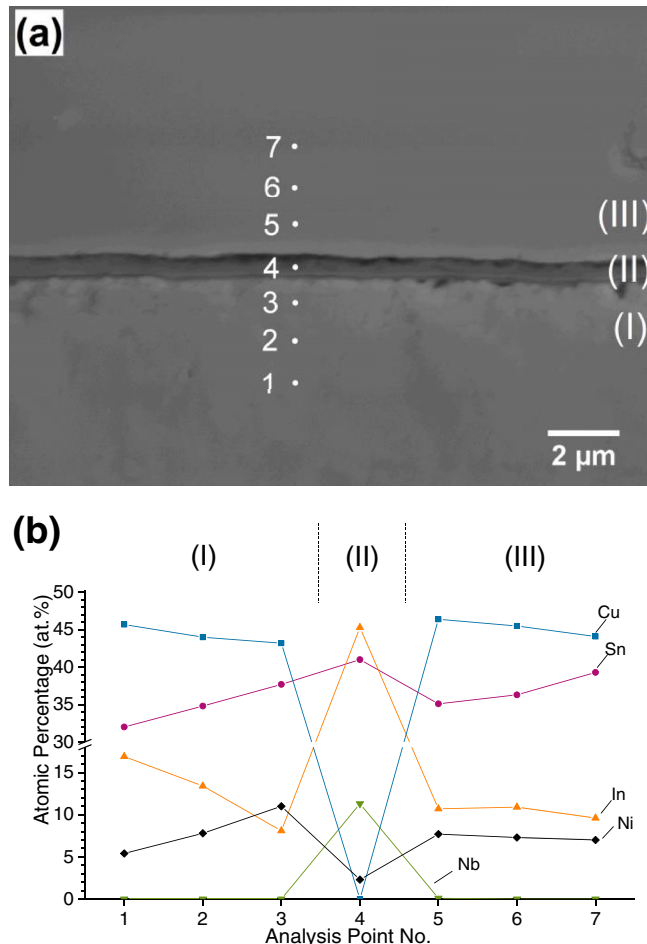


Figure 9. a) SEM image showing the interfacial microstructure of a 94.0Ni-6.0Nb deposited samples after reaction with molten Sn-In solder at 200°C for 9 hours and b) a plot showing the EDX point analysis results indicated in a).

hence did not display any enhanced barrier property (i.e. failed within 3 hours at 200°C). Figure 9 presents the interfacial microstructure of a 2 μm thick, 94.0Ni-6.0NbO $_x$ deposited sample after reaction with molten Sn-In solder at 200°C for 9 hrs, when the Ni-based barrier had been penetrated. Three zones were observed across the interface: I) reacted Cu substrate, II) consumed Ni-NbO $_x$ layer and III) IMCs growing at the solder side. The IMCs in both Zones I and III contained Cu as the effect of the barrier layer had completely diminished. However, it is noteworthy that, the thickness of the barrier layer (Zone II) saw an appreciable reduction from 2 μm to \sim 700 nm after reaction with the molten In-Sn solder, which was accompanied by an increase in the Nb content from 6 to 11 at.%. This is because, following interdiffusion the barrier layer no longer exists in its original form but as a reaction product, where the increased Nb content may simply result from the barrier layer being pushed ahead on the molten reaction front. Moreover, the In content in Zone II was evidently elevated (45 at.%), as compared to that of the adjacent zones (up to 17 at.%), with the atomic ratio of In to Nb at ca. 45:11, which is comparable to that from the 96.8Ni-3.2NbO $_x$ counterpart. This indicates that, reaction of the Ni-NbO $_x$ with molten Sn-In solder forms a layer enriched in Nb and In, with relatively fixed composition (atomic ratio of In to Nb of around 45:10). Such a layer is believed to provide enhanced barrier efficacy presumably by retarding the inter-diffusion of intermetallic forming species (Ni, Sn and In).

Conclusions

Electrodeposition and characterization of Ni-NbO $_x$ composite layers from glycol-based electrolytes consisting of NbCl $_5$, NiCl $_2$ and

propylene glycol have been undertaken to examine the fundamental aspects of this new approach to the development of a Nb-containing diffusion barrier for liquid solder interconnects. With increasing cathodic current density, an increase in the Nb content was generally obtained, which was accompanied by refinement of the deposit surface features. A trade-off between high co-deposited Nb content and large coating thickness was found, as increased NaBH_4 concentrations generally elevated the maximum deposit thickness (above 10 μm) and reduced the co-deposited Nb content. The composite coatings generally exhibited good electrical conductivity as indicated from four-point probe electrical characterization. The reaction behavior between the liquid 52In-48Sn solder and Ni-NbO_x , with Nb contents up to 6 at.%, was investigated at 200°C for up to 2 weeks. Amongst the 7 μm thickness group, the barrier service life was extended from 48 hrs through 72 hrs to 192 hours, when the co-deposited Nb content increased from 0 at.% to 0.6 at.%, and further to 3.2 at.%. Moreover, the Ni-In-Sn IMCs formed at the solder side from the 96.8Nb-3.2NbO_x samples remained adhered to the interface, in contrast to the pure Ni and 99.4Nb-0.6NbO_x where most of the IMCs had spalled into the bulk solder. For the 2 μm thickness, the 94Ni-6NbO_x layer failed within 3 hrs, which is comparable to that of its pure Ni counterpart. The absence of improved barrier efficacy for this high Nb loading sample is thought to be due to small coating thickness as well as to cracks (presumably instigated by interaction with molten solder) providing pathways for ingress of the liquid solder. Nb enrichment, in some cases together with In enrichment, was generally evident at,

or close to, the reaction front between the remaining Ni-based barrier layer and the solder material (i.e. Sn and In). From these results, it is proposed that, the role of Nb as a barrier enhancer presumably arises from its migration (through solid state diffusion) and enrichment at the reaction front, which eventually forms a Nb-enriched zone covering the underlying remaining barrier layer as well as Cu substrate. This is believed to retard the inter-diffusion of IMC forming species (i.e. Ni, In and Sn) and hence to reduce the consumption rate of the Ni-NbO_x diffusion barrier layers.

Acknowledgments

One of us (JW) acknowledge a studentship provided by the Materials Research School at Loughborough University, UK.

References

1. S. H. Mannan and M. P. Clode, *IEEE Trans. Adv. Pack.*, **27**, 508 (2004).
2. S. H. Mannan, M. P. Clode, and M. Dagher, *J. Electron. Mater.*, **34**, 125 (2005).
3. J. Li, S. H. Mannan, M. P. Clode, K. Chen, D. C. Whalley, C. Liu, and D. A. Hutt, *Acta Materialia*, **55**, 737 (2007).
4. K. Chen, C. Liu, D. C. Whalley, D. A. Hutt, J. Li, and S. H. Mannan, *Acta Materialia*, **56**, 5668 (2008).
5. K. Chen, C. Liu, D. C. Whalley, D. A. Hutt, J. Li, and S. H. Mannan In *Proceedings of the 1st Electronics System Integration Technology Conference*, **1**, 421 (2006).
6. J. Wang, G. D. Wilcox, R. J. Mortimer, C. Liu, and M. A. Ashworth, *J. Electrochem. Soc.*, **161**, D395 (2014).
7. C. Y. Huang and S. W. Chen, *J. Electron. Mater.*, **31**, 152 (2002).